

There Is No Free Lunch In Adversarial Robustness (But There Are Unexpected Benefits)

Dimitris Tsipras*
MIT
tsipras@mit.edu

Shibani Santurkar*
MIT
shibani@mit.edu

Logan Engstrom
MIT
engstrom@mit.edu

Alexander Turner
MIT
turneram@mit.edu

Aleksander Madry
MIT
madry@mit.edu

Abstract

We provide a new understanding of the fundamental nature of *adversarially robust* classifiers and how they differ from *standard* models. In particular, we show that there *provably* exists a trade-off between the standard accuracy of a model and its robustness to adversarial perturbations. We demonstrate an intriguing phenomenon at the root of this tension: a certain dichotomy between “robust” and “non-robust” features. We show that while robustness comes at a price, it also has some surprising benefits. Robust models turn out to have interpretable gradients and feature representations that align unusually well with salient data characteristics. In fact, they yield striking feature interpolations that have thus far been possible to obtain only using generative models such as GANs.

1 Introduction

Deep learning models have achieved impressive performance on a number of challenging benchmarks in computer vision, speech recognition and competitive game playing [25, 18, 31, 37, 20]. However, these models turn out to be quite brittle. One can synthesize small, imperceptible perturbations of the input data and cause the model to make highly-confident but erroneous predictions [8, 5, 40].

This problem of so-called *adversarial examples* has garnered significant attention recently and resulted in numerous approaches to both finding these perturbations and to training models that are robust to them [17, 33, 32, 6, 36, 26, 11, 3]. In practice, building such *adversarially robust* models proved to be quite challenging. In particular, many of the proposed defenses were subsequently shown to be ineffective [7, 2, 41]. Only recently, there has been progress towards models that achieve robustness that was demonstrated empirically and, in some cases, even formally verified [30, 23, 39, 34, 21].

The vulnerability of models trained using standard methods to adversarial perturbations makes it clear that the paradigm of adversarially robust model is different to the classic machine learning methodology. In particular, we already know that robustness comes at a cost. This cost takes the form of computationally more expensive training methods (training time) as well as, as shown recently in [35], of the need for more training data. It is natural then to wonder: *Are these the only costs of adversarial robustness?* And, if so, once we choose to pay these costs, *would it always be preferable to have a robust model instead of the standard one?* The goal of this work is to explore these questions and, more broadly, to build a firm understanding of adversarial robustness as a phenomenon.

*Equal Contribution.

Our contributions In this work, we study fundamental properties of adversarially robust classifiers and how they differ from “standard” models, i.e., models that solely aim to maximize the standard accuracy. We prove that there is an inherent trade-off between *standard accuracy* and *adversarial robustness*. Interestingly, this phenomenon persists even in the limit of infinite data and thus demonstrates that resorting to techniques specifically tailored for training robust models might be necessary. This trade-off also explains the decrease in standard accuracy observed when employing adversarial training in practice.

Additionally, we identify an intriguing dichotomy underlying the above phenomena. This dichotomy designates features of a model as either “robust” or “non-robust”, depending on their correlation with the correct classification and their vulnerability to adversarial manipulation. It also suggests alternative methods for training robust classifiers.

Finally, we uncover certain powerful, yet unexpected benefits of adversarially robust models. We find that due to their reliance solely on robust features in the data, these models are more *interpretable* and align well with human perception. In fact, we observe that the feature embeddings learnt by adversarially robust models yield clean manifold interpolations that have thus far been restricted to generative adversarial networks (GANs) [17] and other similar generative models. This hints at existence of a new, deeper connection between GANs and adversarial robustness.

2 Adversarial robustness And robust features

Recall that in the canonical classification setting, the primary focus is on maximizing standard accuracy, i.e. the performance on (yet) unseen samples from the underlying distribution. Specifically, the goal is to train models that have low *expected loss* (also known as population risk):

$$\mathbb{E}_{(x,y) \sim \mathcal{D}} [\mathcal{L}(x, y; \theta)]. \quad (1)$$

Adversarial robustness The existence of adversarial examples largely changed this picture. In particular, there has been a lot of interest in developing models that are resistant to them, or, in other words, models that are *adversarially robust*. In this context, the goal is to train models that have low *expected adversarial loss*:

$$\mathbb{E}_{(x,y) \sim \mathcal{D}} \left[\max_{\delta \in \Delta} \mathcal{L}(x + \delta, y; \theta) \right]. \quad (2)$$

Here, Δ represents the set of perturbations that the adversary can apply to induce misclassification. In this work, we focus on the case when Δ is the set of ℓ_p -bounded perturbations, i.e. $\Delta = \{\delta \in \mathbb{R}^d \mid \|\delta\|_p \leq \varepsilon\}$. This choice is the most common one in the context of adversarial examples and serves as a standard benchmark. It is worth noting though that several other notions of adversarial perturbations have been studied. These include rotations and translations [13, 10], and smooth spatial deformations [44]. In general, determining the “right” Δ to use is a domain specific question.

Adversarial training The most successful approach to building adversarially robust models so far [30, 23, 39, 34, 21] was so-called *adversarial training* [17]. Adversarial training is motivated by viewing (2) as an adversarial generalization statement. This view then suggests that to achieve generalization, we need to solve the corresponding (adversarial) empirical risk minimization problem:

$$\min_{\theta} \mathbb{E}_{(x,y) \sim \widehat{\mathcal{D}}} \left[\max_{\delta \in \mathcal{S}} \mathcal{L}(x + \delta, y; \theta) \right].$$

The resulting saddle point problem can be hard to solve in general. However, it turns out to be often tractable in practice, at least in the context of ℓ_p -bounded perturbations [30, 21]. Specifically, adversarial training corresponds to a natural robust optimization approach to solving this problem [4]. In this approach, we repeatedly find the *worst-case* input perturbations δ (solving the inner maximization problem), and then update the model parameters to reduce the loss on these perturbed inputs.

Even though adversarial training is effective, this success comes with certain drawbacks. The most obvious one is an increase in the training time (we need to compute new perturbations per each parameter update step). The other one corresponds to the potential need for more training data. Specifically, it was recently shown that training adversarially robust models can require significantly

more data [35]. These costs make training more demanding, but is that the whole price of being adversarially robust? In particular, if we are willing to pay these costs: *Are robust classifiers better than standard ones in every other aspect?* This is the key question that motivates our work.

Our point of start is the popular view of adversarial training as the “ultimate” form of data augmentation. According to this view, Δ is seen as the set of invariants that the model should satisfy. Thus, finding the worst-case δ corresponds to augmenting training in the “most-helpful” manner.

A key implication of this view would be that using adversarial training can only *improve* the standard accuracy of a model. This intuition however does not seem to be confirmed in practice [27, 30, 21]. Indeed, in Figure 1 we show the standard accuracy of models trained using adversarial training (with different ℓ_p -bounded adversaries). We observe a steady decline in standard accuracy as the strength of the adversary increases. This observation leads to the question:

Is the decrease in standard accuracy for robust models inevitable?

It turns out that the answer to this question is affirmative. As we will show, there *provably* exists a fundamental trade-off between adversarial robustness and standard accuracy.

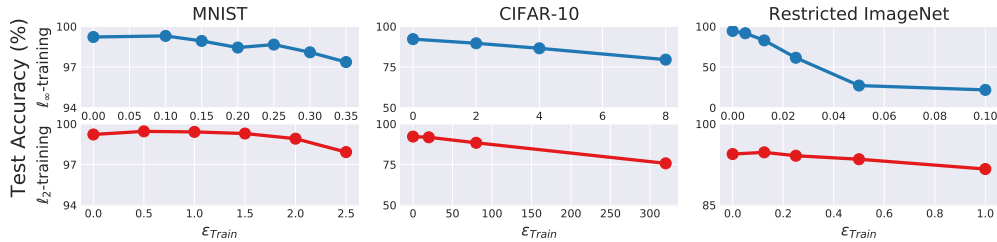


Figure 1: Standard test accuracy of adversarially trained classifiers. The adversary used during training is constrained within some ℓ_p -ball of radius ϵ_{train} (details in Appendix A). We observe a consistent decrease in accuracy as the strength of the adversary increases.

2.1 Adversarial robustness does not come for free

In what follows, we formally show that there is an inherent tension between standard accuracy and adversarial robustness. Surprisingly, this phenomenon seems to be so prevalent that it can be demonstrated even in a fairly simple setting. We introduce this setting below.

Our binary classification task Our data model consists of input-label pairs (x, y) sampled from a distribution \mathcal{D} as follows:

$$y \stackrel{u.a.r.}{\sim} \{-1, +1\}, \quad x_1 = \begin{cases} +y, & \text{w.p. } 0.7 \\ -y, & \text{w.p. } 0.3 \end{cases}, \quad x_2, \dots, x_{d+1} \stackrel{i.i.d.}{\sim} \mathcal{N}(\eta y, 1), \quad (3)$$

where $\mathcal{N}(\mu, \sigma^2)$ is a normal distribution with mean μ and variance σ^2 . We chose η to be large enough so that a simple classifier attains high standard accuracy ($>99\%$) – e.g. $\eta = \Theta(1/\sqrt{d})$ will suffice. The choice of 0.7 is fairly arbitrary; any fixed value in $(0.5, 1)$ will yield qualitatively similar results.

Standard classification is easy Note that samples from \mathcal{D} consist of a single feature that is moderately correlated with the label and d other features that are only *very weakly* correlated with it. Despite the fact that each one of the latter type of features individually is hardly predictive of the correct label, this distribution turns out to be fairly simple to classify from a standard accuracy perspective. Specifically, a natural (linear) classifier

$$f_{\text{avg}}(x) := \text{sign}(w_{\text{unif}}^\top x), \quad \text{where } w_{\text{unif}} := \left[0, \frac{1}{d}, \dots, \frac{1}{d}\right], \quad (4)$$

achieves standard accuracy arbitrarily close to 100%, for d large enough. Indeed, observe that

$$\Pr[f_{\text{avg}}(x) = y] = \Pr[\text{sign}(w_{\text{unif}}^\top x) = y] = \Pr\left[\frac{y}{d} \sum_{i=1}^d \mathcal{N}(\eta y, 1) > 0\right] = \Pr\left[\mathcal{N}\left(\eta, \frac{1}{d}\right) > 0\right],$$

which is $> 99\%$ when $\eta \geq 3/\sqrt{d}$.

Adversarially robust classification Note that in our discussion so far, we effectively viewed the average of x_2, \dots, x_{d+1} as a single “meta-feature” that is highly correlated with the correct label. For a standard classifier, any feature that is even slightly correlated with the label is useful. As a result, a standard classifier will take advantage (and thus rely on) the weakly correlated features x_2, \dots, x_{d+1} (by implicitly pooling information) to achieve almost perfect standard accuracy.

However, this analogy breaks completely in the adversarial setting. In particular, an ℓ_∞ -bounded adversary that is only allowed to perturb each feature by a moderate ε can effectively override the effect of the aforementioned meta-feature. For instance, if $\varepsilon = 2\eta$, an adversary can shift each weakly-correlated feature towards $-y$. The classifier would now see a perturbed input x' such that each of the features x'_2, \dots, x'_{d+1} are sampled i.i.d. from $\mathcal{N}(-\eta y, 1)$ (i.e., now becoming *anti*-correlated with the correct label). Thus, when $\varepsilon \geq 2\eta$, the adversary can essentially simulate the distribution of the weakly-correlated features as if belonging to the wrong class.

Formally, the probability of the meta-feature correctly predicting y in this setting (4) is

$$\min_{\|\delta\|_\infty \leq \varepsilon} \Pr[\text{sign}(x + \delta) = y] = \Pr[\mathcal{N}(\eta, 1) - \varepsilon > 0] = \Pr[\mathcal{N}(-\eta, 1) > 0].$$

As a result, the simple classifier in (4) that relies solely on these features cannot get adversarial accuracy better than 1%.

Intriguingly, this discussion draws a distinction between *robust* features (x_1) and *non-robust* features (x_2, \dots, x_{d+1}) that arises in the adversarial setting. This is caused by the inherent trade-off between a feature’s correlation with the label and its fragility. While the meta-feature is far more predictive of the true label, it is extremely unreliable in the presence of an adversary. Hence, a tension between standard and adversarial accuracy arises. Any classifier that aims for high accuracy (say $> 99\%$) will have to heavily rely on non-robust features (the robust feature provides only 70% accuracy). However, since the non-robust features can be arbitrarily manipulated, this classifier will inevitably have low adversarial accuracy. We make this formal in the following theorem proved in Appendix B.

Theorem 2.1 (No free-lunch in adversarial robustness). *Any classifier that attains at least $1 - \delta$ standard accuracy on \mathcal{D} has adversarial accuracy at most $\frac{7}{3}\delta$ against an ℓ_∞ adversary with $\varepsilon \geq 2\eta$.*

Observe that the above bound implies that as standard accuracy approaches 100% ($\delta \rightarrow 0$), adversarial accuracy falls to 0%. Also it is worth noting that the theorem is tight. If $\delta = 0.3$, both the standard and adversarial accuracies are bounded by 70% which is attained by the classifier that relies solely on the first feature. Additionally, note that compared to the scale of the features ± 1 , the value of ε required to manipulate the standard classifier is very small ($\varepsilon = O(\eta)$).

Finally, we want to emphasize that this separation persists even in the limit of infinite data. The trade-off between standard and adversarial accuracy is an *inherent trait of the data distribution* and not an artifact of having insufficient samples. This result is orthogonal to recent work [35] that demonstrates that vulnerability to adversarial examples can arise due to lack of sufficient samples to reduce the uncertainty about the true distribution.

2.2 The importance of adversarial training

We have now established that a classifier that achieves high standard accuracy (1) will inevitably have very low adversarial accuracy on \mathcal{D} (3). Hence, in an adversarial setting (2), where the goal is to achieve high adversarial accuracy, the training procedure needs to be modified. We now make this phenomenon concrete for linear classifiers trained using the soft-margin SVM loss. Specifically, we present following theorem proved in Appendix C.

Theorem 2.2 (Adversarial training matters). *For $\eta \geq 4/\sqrt{d}$, a soft-margin SVM classifier of unit weight norm minimizing the distributional loss achieves a standard accuracy of $> 99\%$ and adversarial accuracy of $< 1\%$ against an ℓ_∞ -bounded adversary of $\varepsilon \geq 2\eta$. Minimizing the distributional adversarial loss instead leads to a robust classifier that has standard and adversarial accuracy of 70% against any $\varepsilon < 1$.*

This shows that if our focus is on robust models, adversarial training is *essential* in certain settings. Soft-margin SVM classifiers are chosen purely for mathematical convenience. Our proofs do not depend on that in a crucial way and can be adapted, in a straightforward manner, to other natural setting, e.g. logistic regression.

Transferability An interesting implication of our analysis is that standard training produces classifiers that rely on features that are weakly correlated with the correct label. This will be true for any classifier trained on the same distribution. Hence, the adversarial examples that are created by perturbing each feature in the direction of $-y$ will transfer across classifiers trained on independent samples from the distribution. This constitutes an interesting manifestation of the generally observed phenomenon of transferability [40] that might hint at its origin.

2.3 Robust and non-robust features: empirical examination

Our theoretical analysis shows that there is an inherent tension between standard accuracy and adversarial robustness. At the core of our derivation are the concepts of robust and non-robust features. The robustness of a feature is characterized by how strongly it is correlated with the correct label (or it’s negative). It is thus natural to wonder whether these concepts are artifacts of our theoretical analysis or if they manifest more broadly. To this end we perform an exploration of this issue on a real dataset that is amenable to linear classifiers, MNIST [28] (details in Appendix A).

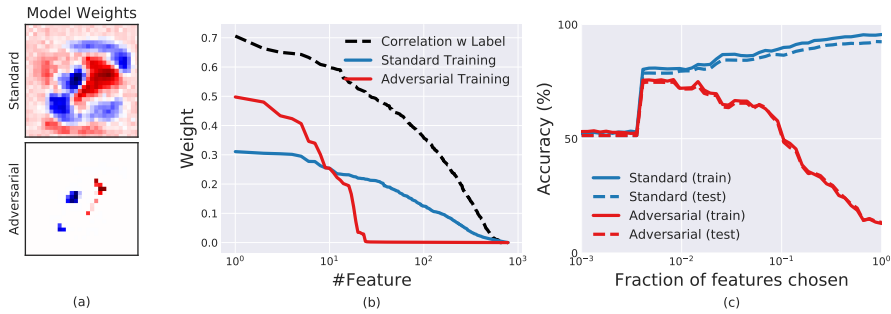


Figure 2: Analysis of linear classifier trained on a binary MNIST task (5 vs. 7). (Details in Appendix Table 4.) (a) Visualization of network weights per input feature. (b) Comparison of feature-label correlation to the weight assigned to the feature by each network. Adversarially trained networks put weights only on a small number of strongly-correlated or “robust” features. (c) Performance of a model trained using *standard* training only on the most robust features. Specifically, we sort features based on decreasing correlation with the label and train using only the most correlated ones. Beyond a certain threshold, we observe that as more non-robust or (weakly correlated) features are available to the model, the standard accuracy increases at the cost of robustness.

Our analysis suggests that, in the adversarial setting, there exists a correlation threshold imposed by the threat model (the amount of perturbation allowed to the adversary). While standard models may utilize all the features with positive correlation, robust models cannot utilize features with correlation below that threshold. We visualize the correlation of each pixel in the MNIST dataset in Figure 2(b). As expected, we observe that the standard classifier assigns weights even to weakly-correlated pixels aiming to improve the confidence of correct prediction, while the robust classifier does not assign any weight below a certain correlation threshold (Figures 2(a, b)).

Interestingly, the standard model assigns non-zero weight even to background image pixels (Figure 2(a)). This suggests that in settings with finite training data, non-robust features could arise from noise. (For instance, in N tosses of an unbiased coin, the expected imbalance between heads and tails is $O(\sqrt{N})$ with high probability.) A standard classifier tries to take advantage of this “hallucinated” information by assigning non-zero weights to these features. This view may suggest that robustness can act as a regularizer, but in practice it appears that this effect is overshadowed by the model’s inability to utilize non-robust features.

An alternative path to robustness The discussion above brings forth a trade-off between predictive power and fragility of features. We wish to examine this phenomenon in more detail. In particular, can test the predictive power of feature correlations? More importantly, can we use these insights to train robust classifiers with standard methods (i.e. without performing adversarial training)? We experiment by training a classifier only on pixels that are above a certain correlation threshold (Figure 2(c)). We find that we can indeed achieve similar performance to adversarial training, suggesting a new, more direct method of training robust networks in certain settings.

3 Unexpected benefits of adversarial robustness

In Section 2 we demonstrated that adversarial robustness has an inherent cost. In particular, we observed that in order to be robust, a classifier must avoid relying on non-robust features, which negatively impacts the standard accuracy of the model. It turns out, however, that relying solely on robust features has unexpected benefits that go beyond robustness, as we illustrate below.

3.1 Robust features align well with salient data characteristics

Given the central role that the dichotomy between robust and non-robust features played in our analysis, one might wonder how these robust features manifest in non-linear settings. A natural approach is to train adversarially robust classifiers for vision datasets and examine the properties of their adversarial examples. Since robust classifiers predominantly rely on robust features, the most impactful way to change their prediction is by perturbing the underlying robust features. We will start from a test image and apply Projected Gradient Descent (PGD; a standard first-order optimization method) to find the image of highest loss within an ℓ_p -ball of radius ε around the original image ².

The resulting visualizations are presented in Figure 3 (details in Appendix A). Strikingly, we can observe that adversarial perturbations for robust models lead to the emergence of prominent characteristics of another class. In fact, the corresponding adversarial examples for robust models often *truly appear* as samples from that class. This behavior is in stark contrast to standard models, for which adversarial examples appear as noisy variants of the input image. Intuitively, this effect stems from the reliance of standard models on the data features that are only weakly predictive of the class.

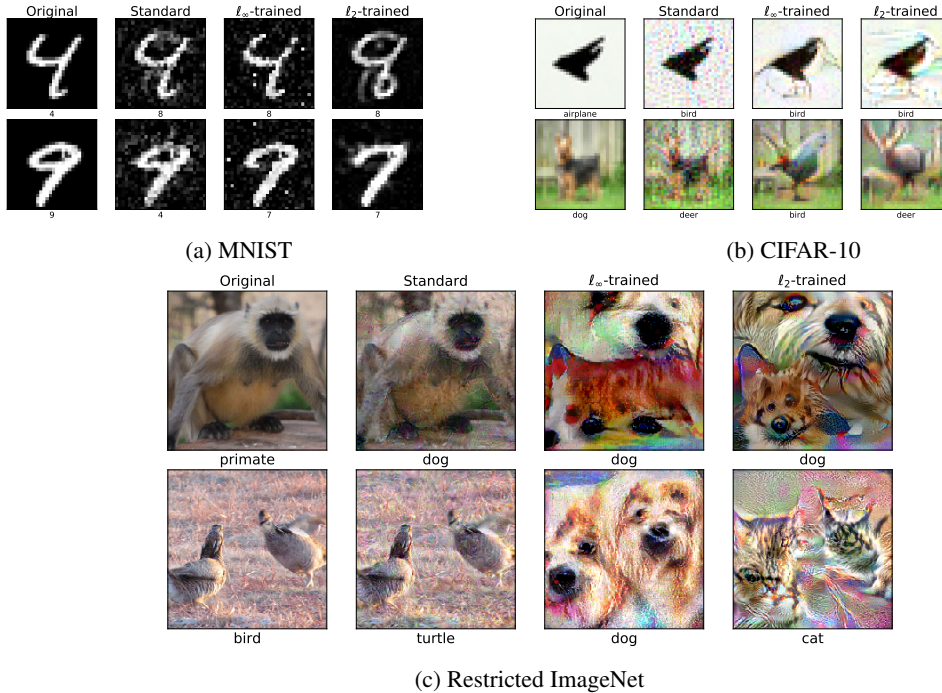


Figure 3: Visualizing large- ε adversarial examples for standard and robust (ℓ_2/ℓ_∞ -adversarial training) models. We construct these examples by iteratively following the (negative) loss gradient while staying with ℓ_2 -distance of ε from the original image. We observe that the images produced for robust models effectively capture salient data characteristics and *truly look* like examples of a different class. (The value of ε is equal for all models and much larger than the one used for training.) Additional examples are visualized in Figure 6 and 7 of Appendix E.

Evidence against gradient masking These findings provide additional evidence that adversarial training does not necessarily lead to gradient obfuscation [2]. Following the gradient changes the

²To allow for significant image changes, we will use much larger values of ε than those used during training.

image in a meaningful way and (eventually) leads to images of different classes. Hence, the robustness of these models does not stem from having gradients that are ill-suited for first-order attacks. Instead it is a result of their invariance to non-robust features.

3.2 GAN-like interpolations via robust features

The strong alignment of robust features with salient data characteristics can be leveraged further. We can linearly interpolate between the original image and the image produce by PGD in Section 3.1 to produce a smooth, “perceptually plausible” interpolation between classes (Figure 4).

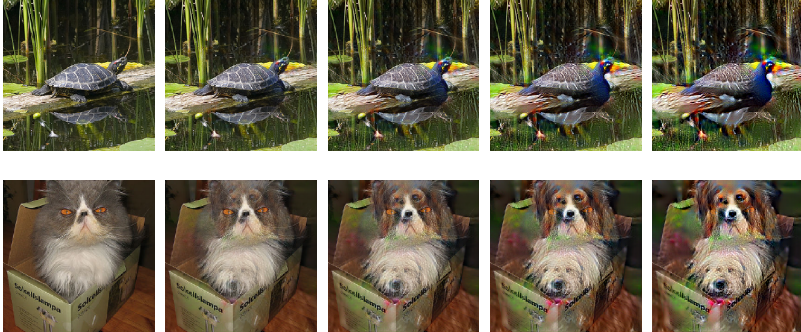


Figure 4: Interpolation between original image and large- ϵ adversarial example as in Figure 3.

The meaningful inter-class manifolds produced by robust networks are reminiscent of the latent space embeddings in GANs [16]. In fact, we conjecture that this similarity is not a coincidence. We postulate that the saddle point problem that is key in both these approaches may be at the root of this effect. We believe that utilizing the loss landscape of robust models will enable powerful interpolations that have thus far been restricted to generative models such as GANs [16] and VAEs [22].

3.3 Robust features as the key to gradient interpretability

It turns out that one can view the previously identified benefits of robust features as the manifestation of a broader phenomenon – gradients of robust models are more *interpretable*. The root of this phenomenon is the fact that the set of perturbations (Δ) encodes a prior for human vision. Adversarial training results in models that are less sensitive to perturbations in Δ . As a result, the gradients of such models will mostly correlate with directions corresponding to perceptual image characteristics.

To illustrate this effect, we visualize the gradients of the loss with respect to individual features (pixels) in the input in Figure 5 (additional visualizations in Figure 8 of Appendix E). We observe that gradients for adversarially trained networks align almost perfectly with perceptually relevant features (such as the boundaries) of the input image. In contrast, for standard networks, these gradients have no coherent patterns and appear to humans as white noise. We want to emphasize that no preprocessing was applied to the gradients (other than scaling and clipping for visualization). So far, extraction of interpretable information from the gradients of trained networks has only been possible with additional involved methods [38, 46].

This new insight on the dependence of classifiers on feature robustness effectively outlines an approach to train models that have interpretable features *by design*. By encoding the correct prior into the set of perturbations Δ , adversarial training alone is sufficient to yield interpretable gradients.

4 Related work

Due to the large body of work on adversarial examples, we will only focus on studies that derive upper bounds for the accuracy of classifiers in the adversarial setting. We defer the full discussion to Appendix D and only present a brief summary here.

We are not aware of any upper bounds on the adversarial robustness of classifiers that: a) are independent of the specific model or model family ([14] and [42] provide bounds for fixed-parameter

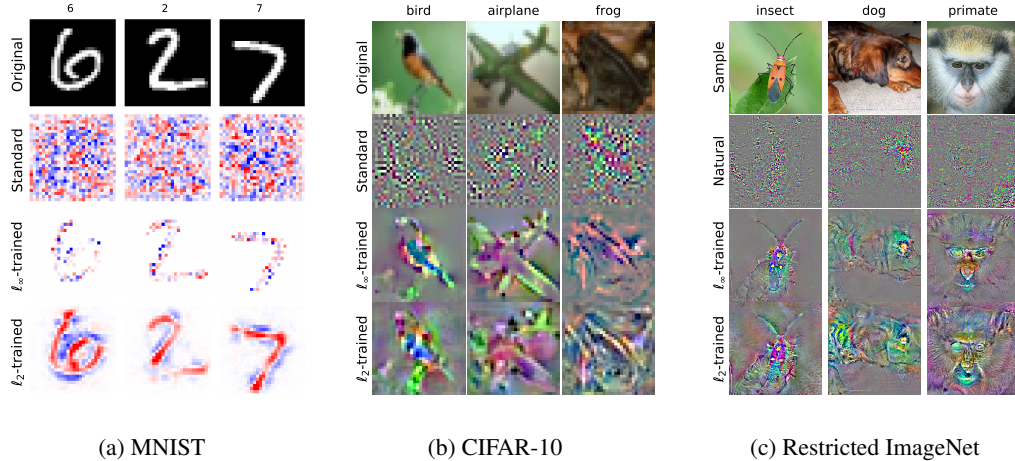


Figure 5: Visualization of the gradient of the loss with respect to input features (pixels). Recall that these gradients highlight the input features which are most strongly correlated with the loss, and thus are the basis for the classifier’s prediction. We observe that the gradients are significantly more *interpretable* for adversarially trained networks – they align almost perfectly with perceptually relevant features. In contrast, for standard networks they look almost like pure noise. (For MNIST, blue and red pixels denote positive and negative gradient regions respectively. For CIFAR and ImageNet, we clip the gradients to within $\pm 3\sigma$ and then rescale them to lie in the $[0, 1]$ range.) Additional visualizations are presented in Figure 8 of Appendix E.

DNNs and k -NN classifiers respectively); b) persist in the limit of infinite data ([15] and [35] rely on finite samples empirically or theoretically); c) separate standard from adversarial training ([12] proves bounds for all classifiers). We believe that our theoretical bounds more accurately capture the situation we face in practice where robust optimization can significantly improve the adversarial robustness of standard classifiers [30, 23, 34, 39]. Moreover, none of these studies prove an inherent trade-off between standard accuracy and adversarial robustness.

5 Conclusions and future directions

In this work, we develop a new understanding of the nature of adversarial robustness, and its relation to classic machine learning setting. In fact, we show that there is no “free lunch” in the adversarial setting, i.e. there *provably* exists a trade-off between standard accuracy and adversarial robustness. This tension stems from an intriguing dichotomy between so-called “robust” and “non-robust” features. This dichotomy does not arise in the classic setting, which provides even more evidence that building robust models, we might require moving away from the canonical classification paradigm. In particular, it might be necessary to employ techniques such as adversarial training.

Even though adversarial robustness comes at a price, it has some unexpected benefits. Robust models turn out to have interpretable gradients and meaningful feature representations that align well with salient data characteristics. The crux of this phenomenon is that the set of adversarial perturbations Δ encodes some prior for human perception. Thus, classifiers that are robust to these perturbations are also necessarily invariant to feature changes that are not fundamentally meaningful.

We demonstrate a striking consequence of this phenomenon: robust models yield feature interpolations that have thus far been possible to obtain only using generative models such as GANs [17]. This emphasizes the possibility of a fundamental connection between GANs and adversarial robustness.

Finally, this new view of robust classifiers suggest an alternative approach to adversarial training. Specifically, we find that standard linear classifiers trained using only robust features match the performance of adversarially trained models. This leaves an interesting possibility: *Could this efficient and interpretable approach to train robust classifiers be extended to general deep networks?* If answered affirmatively, this would constitute the first real alternative to adversarial training.

Acknowledgements

Shibani Santurkar was supported by the National Science Foundation (NSF) under grants IIS-1447786, IIS-1607189, and CCF-1563880, and the Intel Corporation. Dimitris Tsipras was supported in part by the NSF grant CCF-1553428. Aleksander Madry was supported in part by an Alfred P. Sloan Research Fellowship, a Google Research Award, and the NSF grant CCF-1553428.

References

- [1] Tensor flow models repository. <https://github.com/tensorflow/models/tree/master/resnet>, 2017.
- [2] Anish Athalye, Nicholas Carlini, and David Wagner. Obfuscated gradients give a false sense of security: Circumventing defenses to adversarial examples. *arXiv preprint arXiv:1802.00420*, 2018.
- [3] Anish Athalye, Logan Engstrom, Andrew Ilyas, and Kevin Kwok. Synthesizing robust adversarial examples. *arXiv preprint arXiv:1707.07397*, 2017.
- [4] Aharon Ben-Tal, Laurent El Ghaoui, and Arkadi Nemirovski. *Robust optimization*. Princeton University Press, 2009.
- [5] Battista Biggio and Fabio Roli. Wild patterns: Ten years after the rise of adversarial machine learning. *arXiv preprint arXiv:1712.03141*, 2017.
- [6] Nicholas Carlini and David Wagner. Towards evaluating the robustness of neural networks. *arXiv preprint arXiv:1608.04644*, 2016.
- [7] Nicholas Carlini and David Wagner. Adversarial examples are not easily detected: Bypassing ten detection methods. *arXiv preprint arXiv:1705.07263*, 2017.
- [8] Nilesch Dalvi, Pedro Domingos, Mausam, Sumit Sanghai, and Deepak Verma. Adversarial classification. In *International Conference on Knowledge Discovery and Data Mining (KDD)*, 2004.
- [9] J. Deng, W. Dong, R. Socher, L.-J. Li, K. Li, and L. Fei-Fei. ImageNet: A Large-Scale Hierarchical Image Database. In *CVPR09*, 2009.
- [10] Logan Engstrom, Dimitris Tsipras, Ludwig Schmidt, and Aleksander Madry. A rotation and a translation suffice: Fooling cnns with simple transformations. *arXiv preprint arXiv:1712.02779*, 2017.
- [11] Ivan Evtimov, Kevin Eykholt, Earlene Fernandes, Tadayoshi Kohno, Bo Li, Atul Prakash, Amir Rahmati, and Dawn Song. Robust physical-world attacks on machine learning models. *arXiv preprint arXiv:1707.08945*, 2017.
- [12] Alhussein Fawzi, Hamza Fawzi, and Omar Fawzi. Adversarial vulnerability for any classifier. *arXiv preprint arXiv:1802.08686*, 2018.
- [13] Alhussein Fawzi and Pascal Frossard. Manitest: Are classifiers really invariant? In *British Machine Vision Conference (BMVC)*, number EPFL-CONF-210209, 2015.
- [14] Alhussein Fawzi, Seyed-Mohsen Moosavi-Dezfooli, and Pascal Frossard. Robustness of classifiers: from adversarial to random noise. In *Advances in Neural Information Processing Systems*, pages 1632–1640, 2016.
- [15] Justin Gilmer, Luke Metz, Fartash Faghri, Samuel S Schoenholz, Maithra Raghu, Martin Wattenberg, and Ian Goodfellow. Adversarial spheres. *arXiv preprint arXiv:1801.02774*, 2018.
- [16] Ian Goodfellow, Jean Pouget-Abadie, Mehdi Mirza, Bing Xu, David Warde-Farley, Sherjil Ozair, Aaron Courville, and Yoshua Bengio. Generative adversarial nets. In *Advances in neural information processing systems*, pages 2672–2680, 2014.
- [17] Ian J. Goodfellow, Jonathon Shlens, and Christian Szegedy. Explaining and harnessing adversarial examples. *arXiv preprint arXiv:1412.6572*, 2014.
- [18] Alex Graves, Abdel-rahman Mohamed, and Geoffrey Hinton. Speech recognition with deep recurrent neural networks. In *Acoustics, speech and signal processing (icassp), 2013 IEEE international conference on*, pages 6645–6649. IEEE, 2013.
- [19] Kaiming He, Xiangyu Zhang, Shaoqing Ren, and Jian Sun. Deep residual learning for image recognition. *corr abs/1512.03385 (2015)*, 2015.

- [20] Kaiming He, Xiangyu Zhang, Shaoqing Ren, and Jian Sun. Deep residual learning for image recognition. In *Proceedings of the IEEE Conference on Computer Vision and Pattern Recognition*, pages 770–778, 2016.
- [21] Harini Kannan, Alexey Kurakin, and Ian Goodfellow. Adversarial logit pairing. *arXiv preprint arXiv:1803.06373*, 2018.
- [22] Diederik P Kingma and Max Welling. Auto-encoding variational bayes. *arXiv preprint arXiv:1312.6114*, 2013.
- [23] J Zico Kolter and Eric Wong. Provable defenses against adversarial examples via the convex outer adversarial polytope. *arXiv preprint arXiv:1711.00851*, 2017.
- [24] Alex Krizhevsky and Geoffrey Hinton. Learning multiple layers of features from tiny images. 2009.
- [25] Alex Krizhevsky, Ilya Sutskever, and Geoffrey E Hinton. Imagenet classification with deep convolutional neural networks. In *Advances in neural information processing systems*, pages 1097–1105, 2012.
- [26] Alexey Kurakin, Ian Goodfellow, and Samy Bengio. Adversarial examples in the physical world. *arXiv preprint arXiv:1607.02533*, 2016.
- [27] Alexey Kurakin, Ian J. Goodfellow, and Samy Bengio. Adversarial machine learning at scale. *arXiv preprint arXiv:1611.01236*, 2016.
- [28] Yann LeCun, Corinna Cortes, and Christopher J.C. Burges. The mnist database of handwritten digits. Website, 1998.
- [29] Yann LeCun, Corinna Cortes, and CJ Burges. Mnist handwritten digit database. *AT&T Labs [Online]*. Available: <http://yann.lecun.com/exdb/mnist>, 2, 2010.
- [30] Aleksander Madry, Aleksandar Makelov, Ludwig Schmidt, Dimitris Tsipras, and Adrian Vladu. Towards deep learning models resistant to adversarial attacks. *arXiv preprint arXiv:1706.06083*, 2017.
- [31] Volodymyr Mnih, Koray Kavukcuoglu, David Silver, Andrei A Rusu, Joel Veness, Marc G Bellemare, Alex Graves, Martin Riedmiller, Andreas K Fidjeland, Georg Ostrovski, et al. Human-level control through deep reinforcement learning. *Nature*, 518(7540):529, 2015.
- [32] Seyed-Mohsen Moosavi-Dezfooli, Alhussein Fawzi, and Pascal Frossard. Deepfool: A simple and accurate method to fool deep neural networks. In *2016 IEEE Conference on Computer Vision and Pattern Recognition, CVPR 2016, Las Vegas, NV, USA, June 27-30, 2016*, pages 2574–2582, 2016.
- [33] Anh Mai Nguyen, Jason Yosinski, and Jeff Clune. Deep neural networks are easily fooled: High confidence predictions for unrecognizable images. In *IEEE Conference on Computer Vision and Pattern Recognition, CVPR 2015, Boston, MA, USA, June 7-12, 2015*, pages 427–436, 2015.
- [34] Aditi Raghunathan, Jacob Steinhardt, and Percy Liang. Certified defenses against adversarial examples. *arXiv preprint arXiv:1801.09344*, 2018.
- [35] Ludwig Schmidt, Shibani Santurkar, Dimitris Tsipras, Kunal Talwar, and Aleksander Madry. Adversarially robust generalization requires more data. *arXiv preprint arXiv:1804.11285*, 2018.
- [36] Mahmood Sharif, Sruti Bhagavatula, Lujo Bauer, and Michael K. Reiter. Accessorize to a crime: Real and stealthy attacks on state-of-the-art face recognition. In *Proceedings of the 2016 ACM SIGSAC Conference on Computer and Communications Security, Vienna, Austria, October 24-28, 2016*, pages 1528–1540, 2016.
- [37] David Silver, Aja Huang, Chris J Maddison, Arthur Guez, Laurent Sifre, George Van Den Driessche, Julian Schrittwieser, Ioannis Antonoglou, Veda Panneershelvam, Marc Lanctot, et al. Mastering the game of go with deep neural networks and tree search. *nature*, 529(7587):484–489, 2016.
- [38] Karen Simonyan, Andrea Vedaldi, and Andrew Zisserman. Deep inside convolutional networks: Visualising image classification models and saliency maps. *arXiv preprint arXiv:1312.6034*, 2013.
- [39] Aman Sinha, Hongseok Namkoong, and John Duchi. Certifiable distributional robustness with principled adversarial training. *arXiv preprint arXiv:1710.10571*, 2017.
- [40] Christian Szegedy, Wojciech Zaremba, Ilya Sutskever, Joan Bruna, Dumitru Erhan, Ian J. Goodfellow, and Rob Fergus. Intriguing properties of neural networks. *arXiv preprint arXiv:1312.6199*, 2013.

- [41] Jonathan Uesato, Brendan O’Donoghue, Aaron van den Oord, and Pushmeet Kohli. Adversarial risk and the dangers of evaluating against weak attacks. *arXiv preprint arXiv:1802.05666*, 2018.
- [42] Yizhen Wang, Somesh Jha, and Kamalika Chaudhuri. Analyzing the robustness of nearest neighbors to adversarial examples. *arXiv preprint arXiv:1706.03922*, 2017.
- [43] Yuxin Wu et al. Tensorpack. <https://github.com/tensorpack/>, 2016.
- [44] Chaowei Xiao, Jun-Yan Zhu, Bo Li, Warren He, Mingyan Liu, and Dawn Song. Spatially transformed adversarial examples. *arXiv preprint arXiv:1801.02612*, 2018.
- [45] Huan Xu and Shie Mannor. Robustness and generalization. *Machine learning*, 86(3):391–423, 2012.
- [46] Jason Yosinski, Jeff Clune, Anh Nguyen, Thomas Fuchs, and Hod Lipson. Understanding neural networks through deep visualization. *arXiv preprint arXiv:1506.06579*, 2015.

A Experimental setup

A.1 Datasets

We perform our experimental analysis on the MNIST [29], CIFAR-10 [24] and (restricted) ImageNet [9] datasets. For binary classification, we filter out all the images from the MNIST dataset other than the “5” and “7” labelled examples. For the ImageNet dataset, adversarial training is significantly harder since the classification problem is challenging by itself and standard classifiers are already computationally expensive to train. We thus restrict our focus to a smaller subset of the dataset. We group together a subset of existing, semantically similar ImageNet classes into 8 different super-classes, as shown in Table 1. We train and evaluate only on examples corresponding to these classes.

Table 1: Classes used in the Restricted ImageNet model. The class ranges are inclusive.

Class	Corresponding ImageNet Classes
“Dog”	151 to 268
“Cat”	281 to 285
“Frog”	30 to 32
“Turtle”	33 to 37
“Bird”	80 to 100
“Primate”	365 to 382
“Fish”	389 to 397
“Crab”	118 to 121
“Insect”	300 to 319

A.2 Models

- Binary MNIST (Section 2.3): We train a linear classifier with parameters $w \in \mathbb{R}^{784}$, $b \in \mathbb{R}$ on the dataset described in Section A.1 (labels -1 and $+1$ correspond to images labelled as “5” and “7” respectively). We use the cross-entropy loss and perform 100 epochs of gradient descent in training.
- MNIST: We use the simple convolution architecture from the TensorFlow tutorial [1]³.
- CIFAR-10: We consider a standard ResNet model [19]. It has 4 groups of residual layers with filter sizes (16, 16, 32, 64) and 5 residual units each⁴.
- Restricted ImageNet: We use a ResNet-50 [20] architecture using the code from the tensorpack repository [43]. We do not modify the model architecture, and change the training procedure only by changing the number of examples per “epoch” from 1,280,000 images to 76,800 images.

³https://github.com/MadryLab/mnist_challenge/

⁴https://github.com/MadryLab/cifar10_challenge/

A.3 Adversarial training

We perform adversarial training to train robust classifiers following [30]. Specifically, we train against a projected gradient descent (PGD) adversary, starting from a random initial perturbation of the training data. We consider adversarial perturbations in ℓ_p norm where $p = \{2, \infty\}$. Unless otherwise specified, we use the values of ε provided in Table 2 to train/evaluate our models.

Table 2: Value of ε used for adversarial training/evaluation of each dataset and ℓ_p -norm.

Adversary	Binary MNIST	MNIST	CIFAR-10	Restricted Imagenet
ℓ_∞	0.2	0.3	4	0.005
ℓ_2	-	1.5	80	1

A.4 Adversarial examples for large ε

The images we generated for Figure 3 were allowed a much larger perturbation from the original sample in order to produce visible changes to the images. These values are listed in Table 3. Since

Table 3: Value of ε used for large- ε adversarial examples of Figure 3.

Adversary	MNIST	CIFAR-10	Restricted Imagenet
ℓ_∞	0.3	32	0.25
ℓ_2	4	1200	40

these levels of perturbations would allow to truly change the class of the image, training against such strong adversaries would be impossible. Still, we observe that smaller values of ε suffices to ensure that the models rely on the most robust (and hence interpretable) features.

B Proof of Theorem 2.1

The main idea of the proof is that an adversary with $\varepsilon = 2\eta$ is able to change the distribution of features x_2, \dots, x_{d+1} to reflect a label of $-y$ instead of y by subtracting εy from each variable. Hence any information that is used from these features to achieve better standard accuracy can be used by the adversary to reduce adversarial accuracy. We define G_+ to be the distribution of x_2, \dots, x_{d+1} when $y = +1$ and G_- to be that distribution when $y = -1$. We will consider the setting where $\varepsilon = 2\eta$ and fix the adversary that replaces x_i by $x_i - y\varepsilon$ for each $i \geq 2$. This adversary is able to change G_+ to G_- in the adversarial setting and vice-versa.

Consider any classifier $f(x)$ that maps an input x to a class in $\{-1, +1\}$. Let us fix the probability that this classifier predicts class $+1$ for some fixed value of x_1 and distribution of x_2, \dots, x_{d+1} . Concretely, we define p_{ij} to be the probability of predicting $+1$ given that the first feature has sign i and the rest of the features are distributed according to G_j . Formally,

$$\begin{aligned}
p_{++} &= \Pr_{x_2, \dots, x_{d+1} \sim G_+} (f(x) = +1 \mid x_1 = +1), \\
p_{+-} &= \Pr_{x_2, \dots, x_{d+1} \sim G_-} (f(x) = +1 \mid x_1 = +1), \\
p_{-+} &= \Pr_{x_2, \dots, x_{d+1} \sim G_+} (f(x) = +1 \mid x_1 = -1), \\
p_{--} &= \Pr_{x_2, \dots, x_{d+1} \sim G_-} (f(x) = +1 \mid x_1 = -1).
\end{aligned}$$

Using these definitions, we can express the standard accuracy of the classifier as

$$\begin{aligned}
\Pr(f(x) = y) &= \Pr(y = +1) (0.7p_{++} + 0.3p_{-+}) \\
&\quad + \Pr(y = -1) (0.7(1 - p_{--}) + 0.3(1 - p_{+-})) \\
&= \frac{1}{2} (0.7p_{++} + 0.3p_{-+} + 0.7(1 - p_{--}) + 0.3(1 - p_{+-})) \\
&= \frac{1}{2} (0.7(1 + p_{++} - p_{--}) + 0.3(1 + p_{-+} - p_{+-})).
\end{aligned}$$

Similarly, we can express the accuracy of this classifier against the adversary that replaces G_+ with G_- (and vice-versa) as

$$\begin{aligned}
\Pr(f(x_{\text{adv}}) = y) &= \Pr(y = +1) (0.7p_{+-} + 0.3p_{--}) \\
&\quad + \Pr(y = -1) (0.7(1 - p_{-+}) + 0.3(1 - p_{++})) \\
&= \frac{1}{2} (0.7p_{+-} + 0.3p_{--} + 0.7(1 - p_{-+}) + 0.3(1 - p_{++})) \\
&= \frac{1}{2} (0.7(1 + p_{+-} - p_{-+}) + 0.3(1 + p_{--} - p_{++})).
\end{aligned}$$

For convenience we will define $a = 1 - p_{++} + p_{--}$ and $b = 1 - p_{-+} + p_{+-}$. Then we can rewrite

$$\begin{aligned}
\text{standard accuracy : } & \frac{1}{2} (0.7(2 - a) + 0.3(2 - b)) \\
&= 1 - \frac{1}{2} (0.7a + 0.3b), \\
\text{adversarial accuracy : } & \frac{1}{2} (0.3a + 0.7b).
\end{aligned}$$

We are assuming that the standard accuracy of the classifier is at least $1 - \delta$ for some small δ . This implies that

$$1 - \frac{1}{2} (0.7a + 0.3b) \geq 1 - \delta \implies 0.7a + 0.3b \leq 2\delta.$$

Since p_{ij} are probabilities, we can guarantee that $a \geq 0$. We use this to upper bound the adversarial accuracy by

$$\begin{aligned}
\frac{1}{2} (0.3a + 0.7b) &\leq \frac{1}{2} \left(0.3 \frac{49}{9} a + 0.7b \right) \\
&= \frac{0.7}{0.6} (0.7a + 0.3b) \\
&\leq \frac{7}{3} \delta.
\end{aligned}$$

□

C Proof of Theorem 2.2

We consider the problem of fitting the distribution \mathcal{D} of (3) by using a standard soft-margin SVM classifier. Specifically, this can be formulated as:

$$\min_w \mathbb{E}[\max(0, 1 - yw^\top x)] + \frac{1}{2} \lambda \|w\|_2^2 \quad (5)$$

for some value of λ . We will assume that we tune λ such that the optimal solution w^* has ℓ_2 -norm of 1. This is without much loss of generality since our proofs can be adapted to the general case. We will refer to the first term of (5) as the *margin* term and the second term as the *regularization* term.

First we will argue that, due to symmetry, the optimal solution will assign equal weight to all the features x_i for $i = 2, \dots, d+1$.

Lemma C.1. *Consider an optimal solution w^* to the optimization problem (5). Then,*

$$w_i^* = w_j^* \quad \forall i, j \in \{2, \dots, d+1\}.$$

Proof. Assume that $\exists i, j \in \{2, \dots, d+1\}$ such that $w_i^* \neq w_j^*$. Since the distribution of x_i and x_j are identical, we can swap the value of w_i and w_j , to get an alternative set of parameters \hat{w} that has the same loss function value ($\hat{w}_j = w_i$, $\hat{w}_i = w_j$, $\hat{w}_k = w_k$ for $k \neq i, j$).

Moreover, since the margin term of the loss is convex in w , using Jensen's inequality, we get that averaging w^* and \hat{w} will not increase the value of that margin term. Note, however, that $\|\frac{w^* + \hat{w}}{2}\|_2 < \|w^*\|_2$, hence the regularization loss is strictly smaller for the average point. This contradicts the optimality of w^* . \square

Since every optimal solution will assign equal weight to all x_i for $k \geq 2$, we can replace these features by their sum (and divide by \sqrt{d} for convenience). We will define

$$z = \frac{1}{\sqrt{d}} \sum_{i=2}^{d+1} x_i,$$

which, by the properties of the normal distribution, is distributed as

$$z \sim \mathcal{N}(y\eta\sqrt{d}, 1).$$

By assigning a weight of v to that combined feature the optimal solutions can be parametrized as

$$w^\top x = w_1 x_1 + v z,$$

where the regularization term of the loss is $\lambda(w_1^2 + v^2)/2$.

Recall that our chosen value of η is $4/\sqrt{d}$, which implies that the contribution of vz is distributed normally with mean $4yv$ and variance v^2 . By the concentration of the normal distribution, the probability of vz being larger than v is large. We will use this fact to show that the optimal classifier will assign on v at least as much weight as it assigns on w_1 .

Lemma C.2. *Consider the optimal solution (w_1^*, v^*) of the problem (5). Then*

$$v^* \geq \frac{1}{\sqrt{2}}.$$

Proof. Assume for the sake of contradiction that $v^* < 1/\sqrt{2}$. Then, with probability at least 0.3, the first feature predicts the wrong label and without enough weight, the remaining features cannot compensate for it. Concretely,

$$\begin{aligned} \mathbb{E}[\max(0, 1 - yw^\top x)] &\geq 0.3 \mathbb{E}[\max(0, 1 + w_1 - \mathcal{N}(4v, v^2))] \\ &\geq 0.3 \mathbb{E}\left[\max\left(0, 1 + \frac{1}{\sqrt{2}} - \mathcal{N}\left(\frac{4}{\sqrt{2}}, \frac{1}{2}\right)\right)\right] \\ &> 0.005. \end{aligned}$$

We will now show that a solution that assigns zero weight on the first feature ($v = 1$ and $w_1 = 0$), achieves a better margin loss.

$$\begin{aligned} \mathbb{E}[\max(0, 1 - yw^\top x)] &= \mathbb{E}[\max(0, 1 - \mathcal{N}(4, 1))] \\ &< 0.0004. \end{aligned}$$

Since both solutions have the same norm, the solution that assigns weight only on v is better than the original solution (w_1^*, bv^*) , contradicting its optimality. \square

We have established that the learned classifier will assign more weight to v than w_1 . Since z will be at least y with large probability, we will show that the behavior of the classifier depends entirely on z .

Lemma C.3. *The standard accuracy of the soft-margin SVM learned for problem (5) is at least 99%.*

Proof. By Lemma C.2, the classifier predicts the sign of $w_1x_1 + vz$ where $vz \sim \mathcal{N}(4yv, v^2)$ and $v \geq 1/\sqrt{2}$. Hence with probability at least 99%, $vzy > 1/\sqrt{2} \geq w_1$ and thus the predicted class is y (the correct class) independent of x_1 . \square

We can utilize the same argument to show that an adversary that changes the distribution of z has essentially full control over the classifier prediction.

Lemma C.4. *The adversarial accuracy of the soft-margin SVM learned for (5) is at most 1% against an ℓ_∞ -bounded adversary of $\varepsilon = 2\eta$.*

Proof. Observe that the adversary can shift each feature x_i towards y by 2η . This will cause z to be distributed as

$$z_{\text{adv}} \sim \mathcal{N}(-y\eta\sqrt{d}, 1).$$

Therefore with probability at least 99%, $vzy < -y \leq -w_1$ and the predicted class will be $-y$ (wrong class) independent of x_1 . \square

It remains to show that adversarial training for this classification task with $\varepsilon > 2\eta$ will result in a classifier that relies solely on the first feature.

Lemma C.5. *Minimizing the adversarial variant of the loss (5) results in a classifier that assigns 0 weight to features x_i for $i \geq 2$.*

Proof. The optimization problem that adversarial training solves is

$$\min_w \max_{\|\delta\|_\infty \leq \varepsilon} \mathbb{E}[\max(0, 1 - yw^\top x)] + \frac{1}{2}\lambda\|w\|_2^2,$$

which is equivalent to

$$\min_w \mathbb{E}[\max(0, 1 - yw^\top x + \varepsilon\|w\|_1)] + \frac{1}{2}\lambda\|w\|_2^2.$$

Consider any optimal solution w for which $w_i > 0$ for some $i > 2$. The contribution of terms depending on w_i to $1 - yw^\top x + \varepsilon\|w\|_1$ is a normally-distributed random variable with mean $2\eta - \varepsilon \leq 0$. Since the mean is non-positive, setting w_i to zero can only decrease the margin term of the loss. At the same time, setting w_i to zero *strictly* decreases the regularization term, contradicting the optimality of w . \square

Clearly, such a classifier will have standard and adversarial accuracy of 70% against any $\varepsilon < 1$ since such a value of ε is not sufficient to change the sign of the first feature. This concludes the proof of the theorem.

D Related work

Wang et al. [42] analyze the adversarial robustness of nearest neighbor classifiers. Instead we focus on lower bounds that are inherent to the statistical setting itself and apply to all classifiers.

Schmidt et al. [35] study the generalization aspect of adversarial robustness. They show that the number of samples needed to achieve adversarially robust generalization is polynomially larger in the dimension than the number of samples needed to ensure standard generalization. In the limit of infinite samples, a simple linear classifier can achieve perfect standard and adversarial accuracy. In contrast, our results are orthogonal and capture the optimization aspect of the problem, persisting in the limit of infinite data. We show that fundamentally different classifiers are needed to achieve high accuracy in the adversarial setting.

Fawzi et al. [14] derive parameter-dependent bounds on the robustness of any fixed classifier. Our results focus on the statistical setting itself and provide lower bounds for *all* classifiers learned in this setting.

Gilmer et al. [15] demonstrate a setting where even a small amount of standard error implies that most points provably have a misclassified point close to them. In this setting, achieving perfect standard accuracy (easily achieved by a simple classifier) is sufficient to achieve perfect adversarial

robustness. In contrast, our work focuses on a setting where adversarial training (provably) matters and there exists a trade-off between standard and adversarial accuracy. We believe that this captures more closely the situation faced in practice.

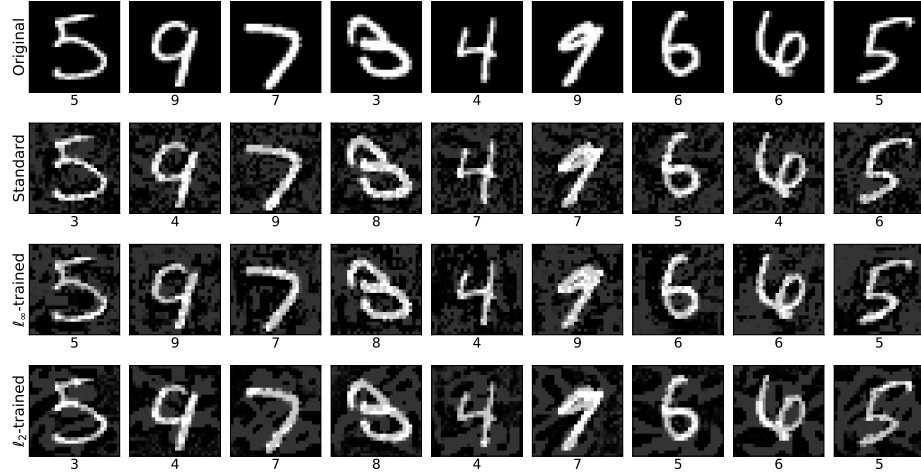
Xu and Mannor [45] explore the connection between robustness and generalization, showing that, in a certain sense, robustness can imply generalization. This direction is orthogonal to our, since we work in the limit of infinite data, optimizing the distributional loss directly.

Fawzi et al. [12] prove lower bounds on the robustness of any classifier based on certain generative assumptions. Since these bounds apply to all classifiers, independent of architecture and training procedure, they fail to capture the situation we face in practice where robust optimization can significantly improve the adversarial robustness of standard classifiers [30, 23, 34, 39].

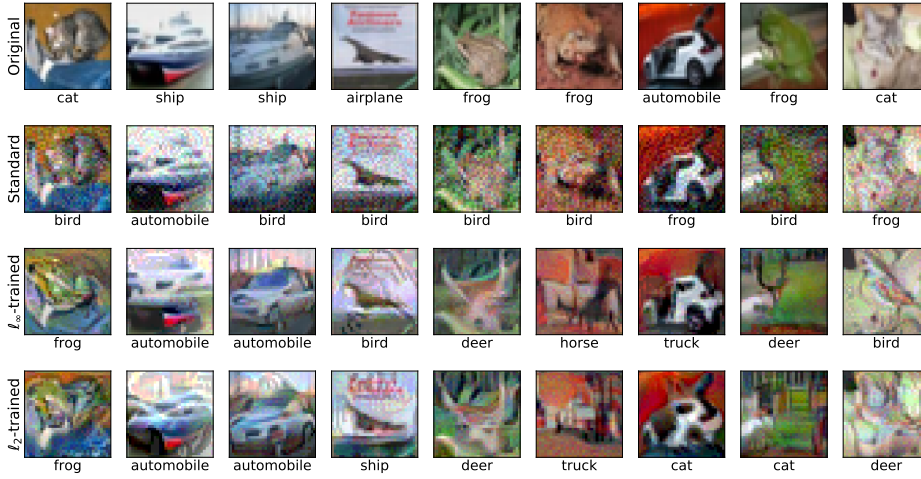
E Omitted figures

Table 4: Comparison of performance of linear classifiers trained on a binary MNIST dataset with standard and adversarial training. The performance of both models is evaluated in terms of standard and adversarial accuracy. Adversarial accuracy refers to the percentage of examples that are correctly classified after being perturbed by the adversary. Here, we use an ℓ_∞ threat model with $\varepsilon = 0.20$ (with images scaled to have coordinates in the range $[0, 1]$).

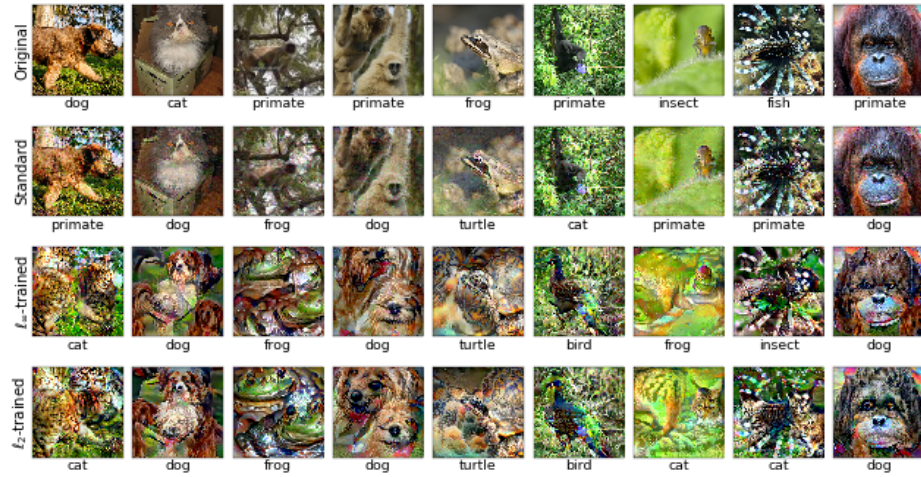
	Standard Accuracy (%)		Adversarial Accuracy (%)		$\ w\ _1$
	Train	Test	Train	Test	
Standard Training	98.38	70.05	13.69	14.95	41.08
Adversarial Training	94.05	92.10	76.05	74.65	13.69



(a) MNIST

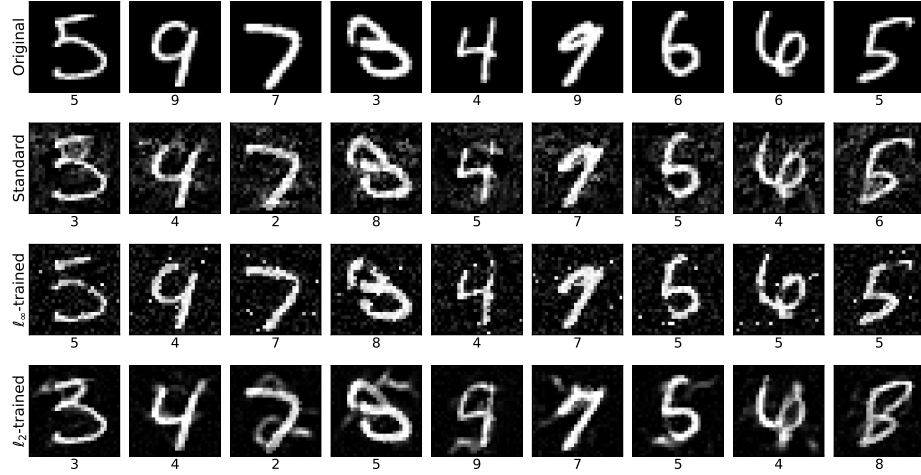


(b) CIFAR-10

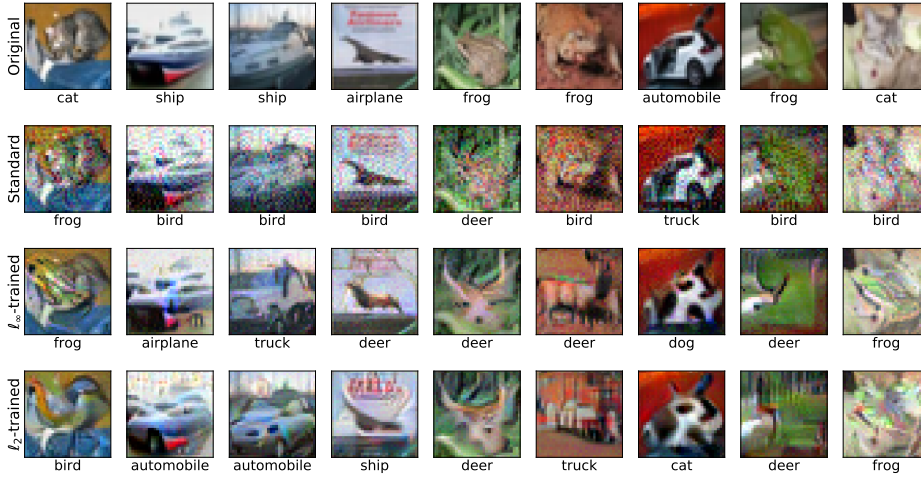


(c) Restricted ImageNet

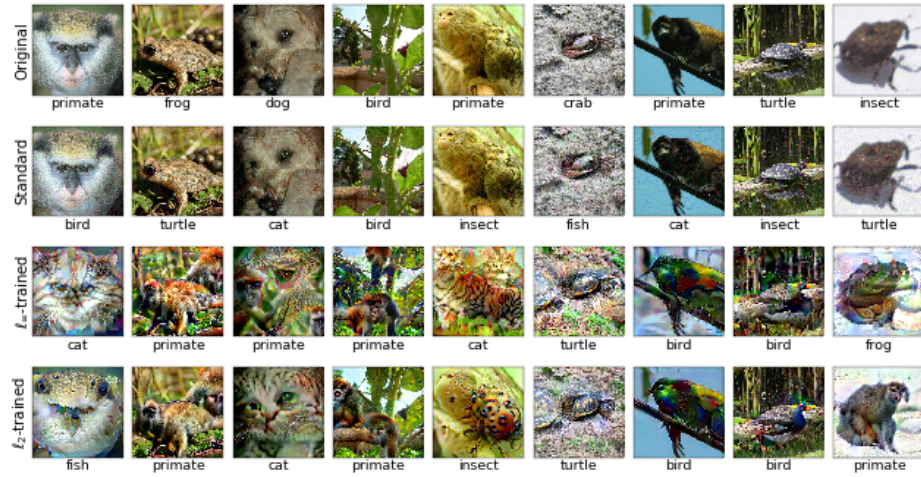
Figure 6: Large- ε adversarial examples, bounded in ℓ_∞ -norm, similar to those in Figure 3. (Low ImageNet resolutions due to file size constraints.)



(a) MNIST

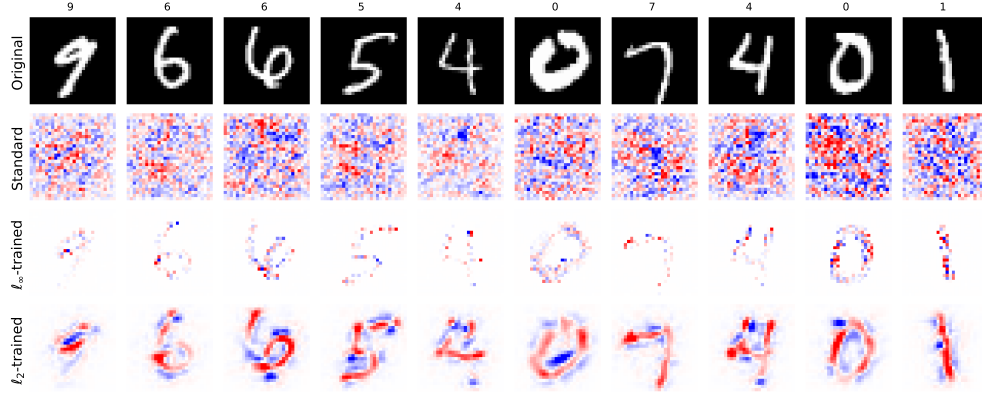


(b) CIFAR-10

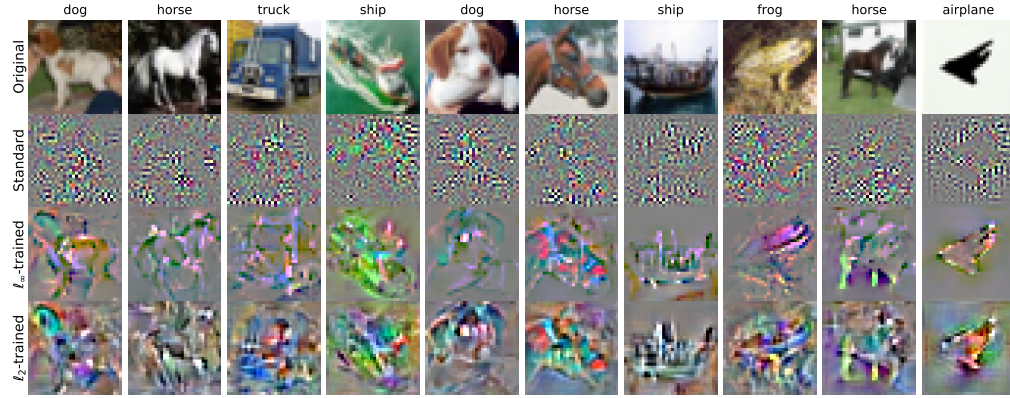


(c) Restricted ImageNet

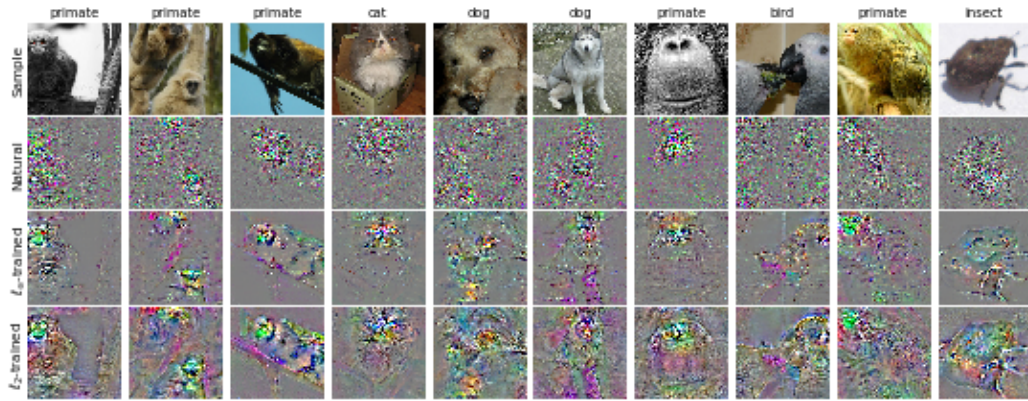
Figure 7: Large- ε adversarial examples, bounded in l_2 -norm, similar to those in Figure 3. (Low ImageNet resolutions due to file size constraints.)



(a) MNIST



(b) CIFAR-10



(c) Restricted ImageNet

Figure 8: Visualization of the gradient of the loss with respect to input features (pixels) for standard and adversarially trained networks for 10 randomly chosen samples, similar to those in Figure 5. Gradients are significantly more *interpretable* for adversarially trained networks – they align almost perfectly with perceptually relevant features. For MNIST, blue and red pixels denote positive and negative gradient regions respectively. For CIFAR10 and Restricted ImageNet we clip pixel to 3 standard deviations and scale to $[0, 1]$. (Low ImageNet resolution due to file size constraints.)